Electronic Supplementary Material (ESI) for Journal of Materials Chemistry A.

Understanding the role of lithium sulfide clusters in lithium-sulfur battery

Tong Yu[1], Fei Li[1], Chunyu Liu[1], Shoutao Zhang[1], Haiyang Xu[1,*] and Guochun Yang[1,2,*]

1. Centre for Advanced Optoelectronic Functional Materials Research and Key Laboratory for UV Light-Emitting Materials and Technology of Ministry of Education, Northeast Normal University, Changchun 130024, China

2. State Key Laboratory of Superhard Materials, Jilin University, Changchun 130012, China

Contents

1. Computational Details·····**3**

2. The structures of the considered anchoring materials·····**5**

3. The comparison of the binding energy per atom·····**6**

4. Adsorption configurations on graphene·····**7**

5. Adsorption configurations on B-doped graphene and N-doped graphene at 1% doped concentration·····**8**

6. Adsorption configurations on B-doped graphene and N-doped graphene at 3.1% doped concentration·····**10**

7. Adsorption configurations on B-doped graphene and N-doped graphene at 5.2% doped concentration·····**12**

8. The adsorption energy (E_a) variations of Li_2S, $(Li_2S)_4$ and $(Li_2S)_8$ on B-doped graphene and N-doped graphene at different doped concentrations·····**14**

9. The calculated charge density difference·····**14**

10. The simulated infrared absorption spectra·····**15**

11. The comparison between the simulated infrared absorption (IR) and Raman spectra·····**16**

12. The HOMO-LUMO gap (energy gap) as a function of cluster size *n*·····**17**

13. Cartesian coordinates of $(Li_2S)_n$ (n = 1 - 10) at B3LYP/6-31G+(*d*) level·····**17**

14. References·····**22**

1. Computational Details

Our structural prediction approach is based on a global minimization of free energy surfaces merging *ab initio* total-energy calculations with CALYPSO (Crystal structure AnaLYsis by Particle Swarm Optimization) methodology as implemented in the CALYPSO code.[1,2] In the first step, random structures of the considered clusters are constructed. Local optimizations using the Gaussian 09 program package[3] were done at B3LYP/3-21G* for Li and 6-31G for S atoms level of theory. After processing the first generation structures, 60% of them with lower Gibbs free energies are selected to construct the next generation structures by PSO (Particle Swarm Optimization). 40% of the structures in the new generation are randomly generated. A structure fingerprinting technique of bond characterization matrix is applied to the generated structures, so that identical structures are strictly forbidden. These procedures significantly enhance the diversity of the structures, which is crucial for structural global search efficiency. In most cases, structural searching simulations for each calculation were stopped after generating 1000 ~ 1200 structures (e.g., about 20 ~ 30 generations).

To further analyze the structures with higher accuracy, we select a number of structures with lower Gibbs free energies and perform structural optimization at B3LYP/6-31+G(*d*) level of theory. With the only input of chemical compositions in our CALYPSO structure searching calculations, the experimental structure of Li_2S with C_{2v} symmetry was successfully reproduced, validating our structure searching methodology in application to the studied system.

To test the suitability of B3LYP/6-31+G(*d*) for $(Li_2S)_n$ clusters, Five DFT functionals and six basis sets were used. Here, $(Li_2S)_4$ was taken as an example. The calculated results were shown Tables S0 and S01. These results indicate that Li-S bond length is not sensitive the selected functionals and basis sets (e.g. the maximum bond length deviation is only 0.02 Å). In addition, our calculated Li-S bond length in Li_2S monomer is 2.10 Å, at B3LYP/6-31+G(d) level, which is good agreement with the recent report value of 2.09 Å [*Nano Eenrgy* **2016**, *25*, 203.] and 2.10 Å [*Phys.*

Chem. Chem. Phys., 2015, **17**, 9032]. B3LYP functional have also widely used to calculate lithium polysulfide species [*Phys. Chem. Chem. Phys.* 2014, 16, 10923; *J. Phys. Chem. C* 2014, 118, 11545; *J. Energy. Chem.* 2013, 22, 72].

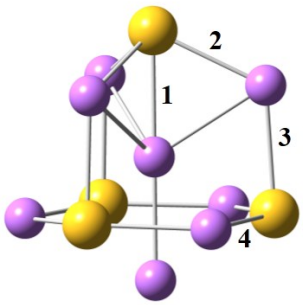

Figure S0. The selected unequal bond lengths in $(Li_2S)_4$. $(Li_2S)_4$ has C_{3v} symmetry.

Table S0. The calculated Li-S bond lengths (in Å) of $(Li_2S)_4$ used B3LYP functional with six different basis sets.

Basis sets	Bond 1	Bond 2	Bond 3	Bond 4
6-31G(d)	2.32	2.30	2.37	2.31
6-31+G(d)	2.32	2.30	2.37	2.30
6-31G(2df,p)	2.31	2.28	2.35	2.28
6-311G(3df)	2.31	2.30	2.35	2.29
6-311++G(d,p)	2.30	2.29	2.36	2.29
6-311++G(2df,p)	2.31	2.29	2.35	2.29

Table S01. The calculated Li-S bond lengths (in Å) of $(Li_2S)_4$ used different functionals with 6-31+G(d) basis set.

Functional	Bond 1	Bond 2	Bond 3	Bond 4
B3LYP	2.31	2.28	2.35	2.28
PBE1PBE	2.30	2.28	2.34	2.28
CAM-B3LYP	2.29	2.27	2.33	2.27
M05-2X	2.31	2.29	2.36	2.29
BHandHLYP	2.29	2.27	2.34	2.27

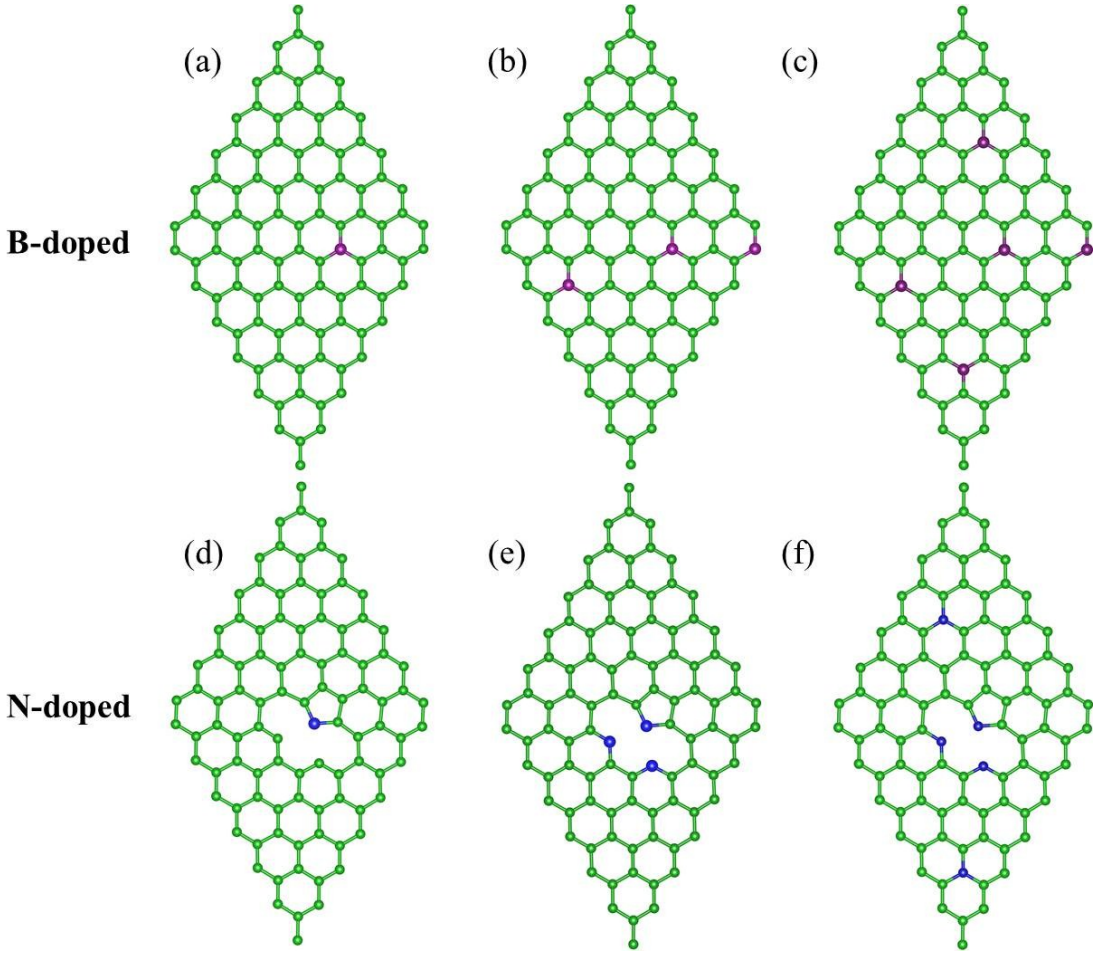

Figure S01. The structures of B-doped graphene and B-doped graphene. From left to right, the doping concentrations were 1%, 3.1% and 5.2%, respectively.

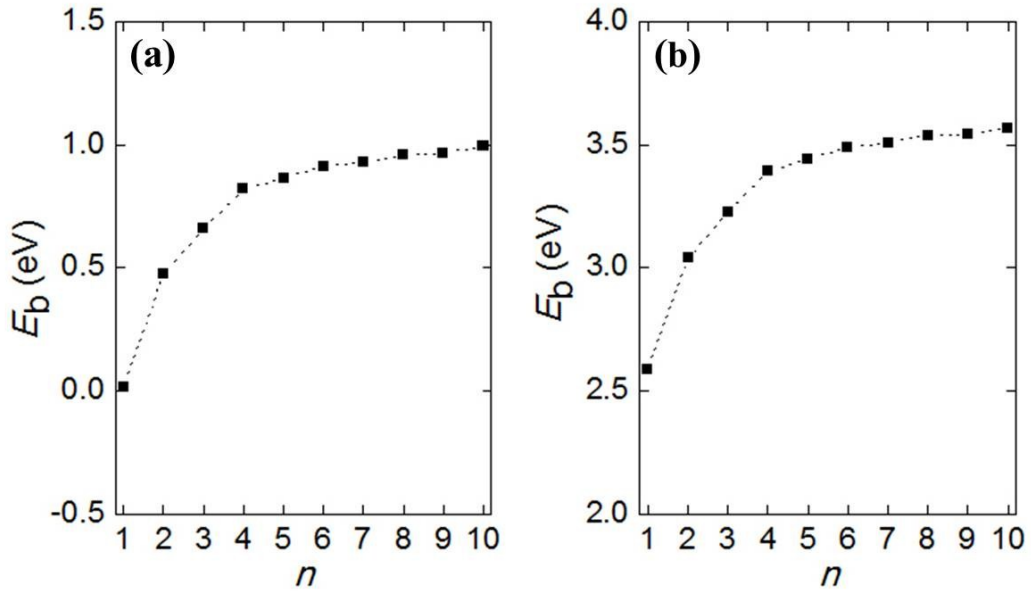

Figure S1. The comparison of the binding energy per atom (E_b) between the two different referred matters. (a) E_b was calculated by bulk Li and S_8. (b) E_b was obtained through single S and Li atoms.

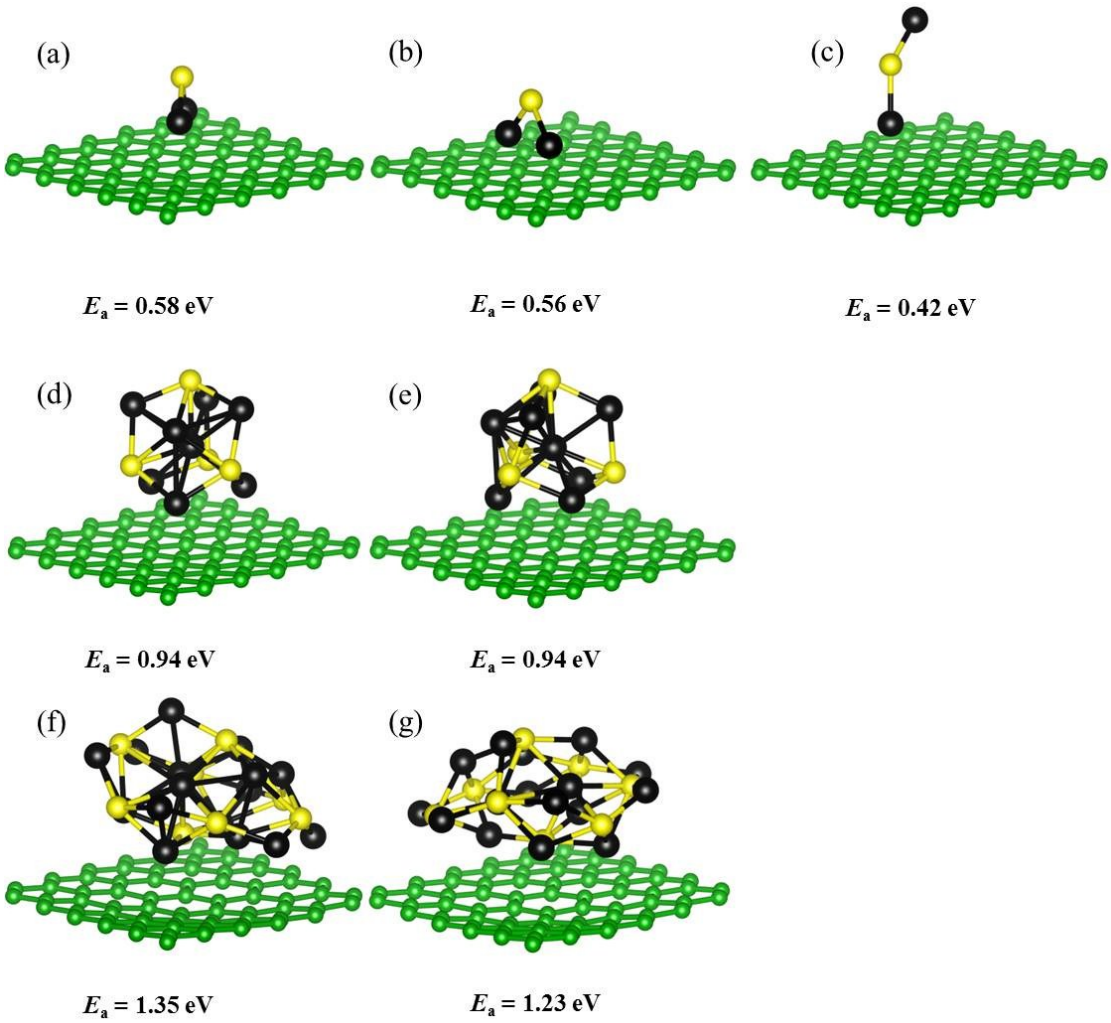

Figure S2. Adsorption configurations and their corresponding adsorption energies on graphene substrate.

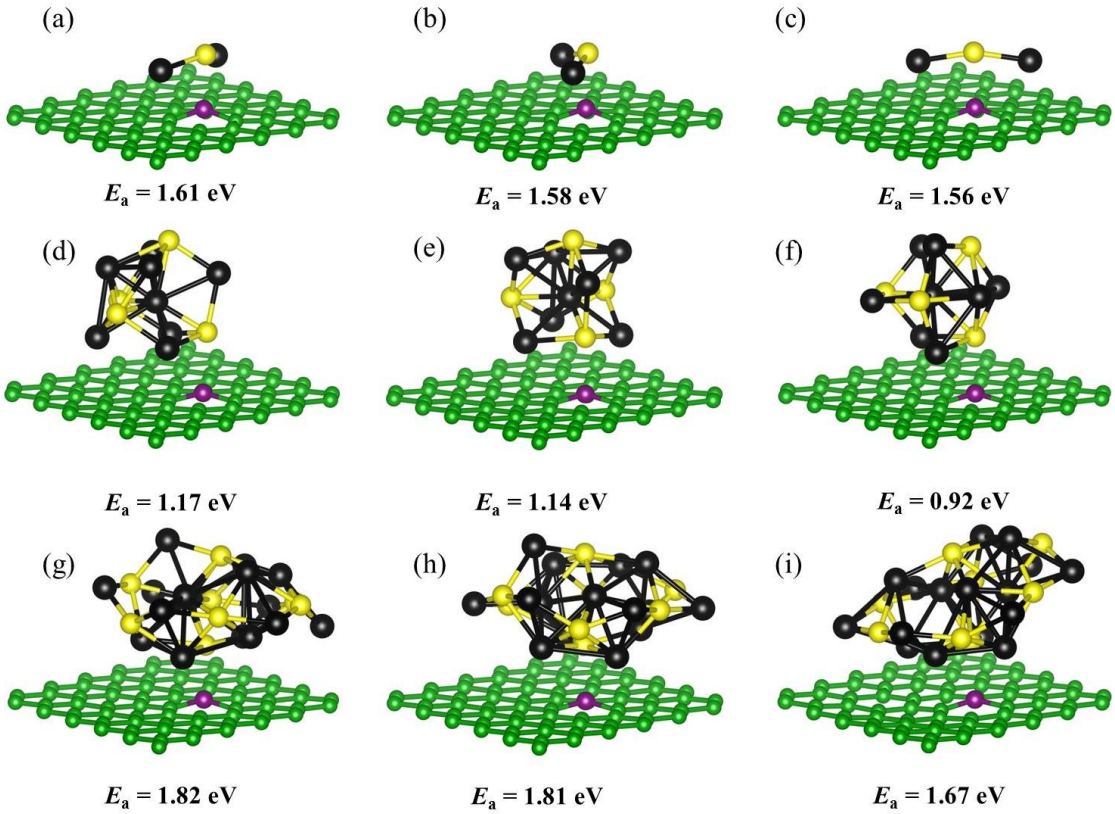

Figure S3. Adsorption configurations and their corresponding adsorption energies on B-doped graphene with 1% concentration.

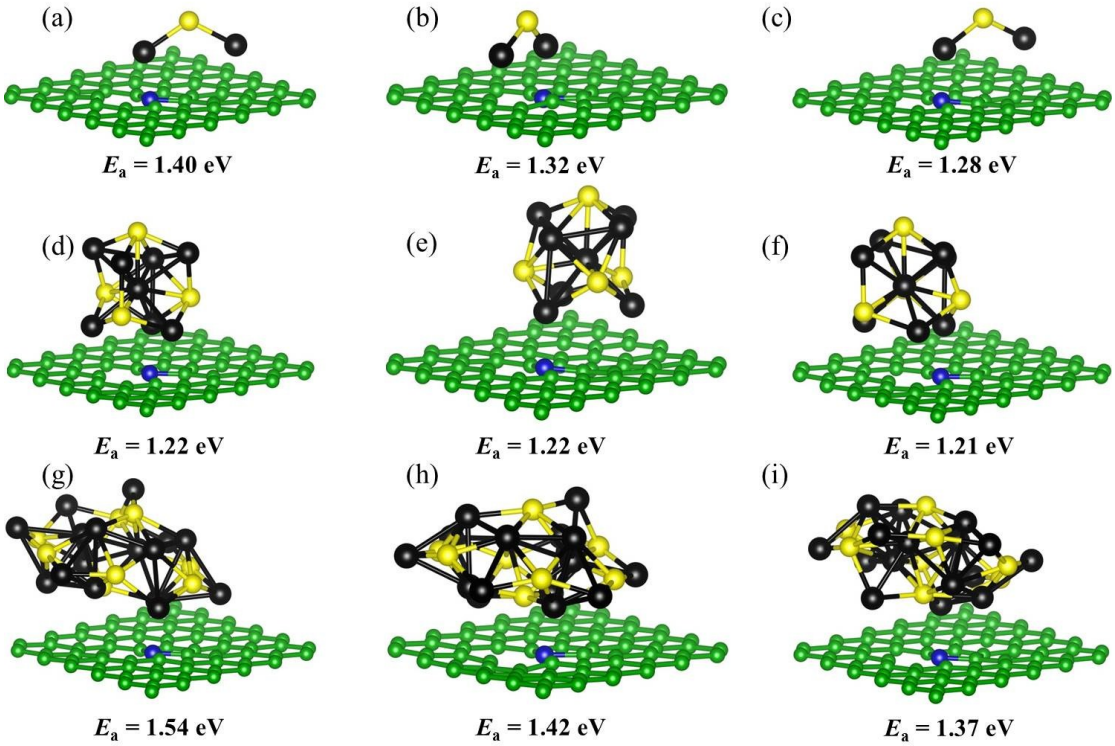

Figure S4. Adsorption configurations and their corresponding adsorption energies on N-doped graphene with 1% concentration.

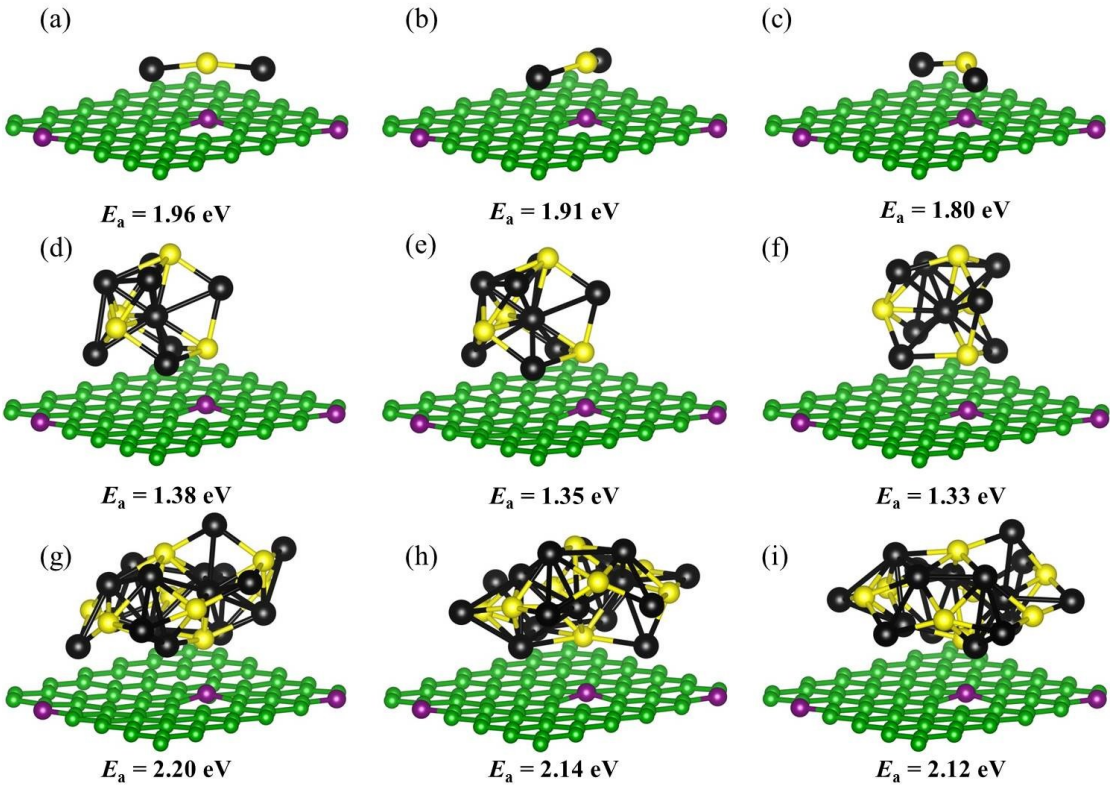

Figure S5. Adsorption configurations and their corresponding adsorption energies on B-doped graphene with 3.1% concentration.

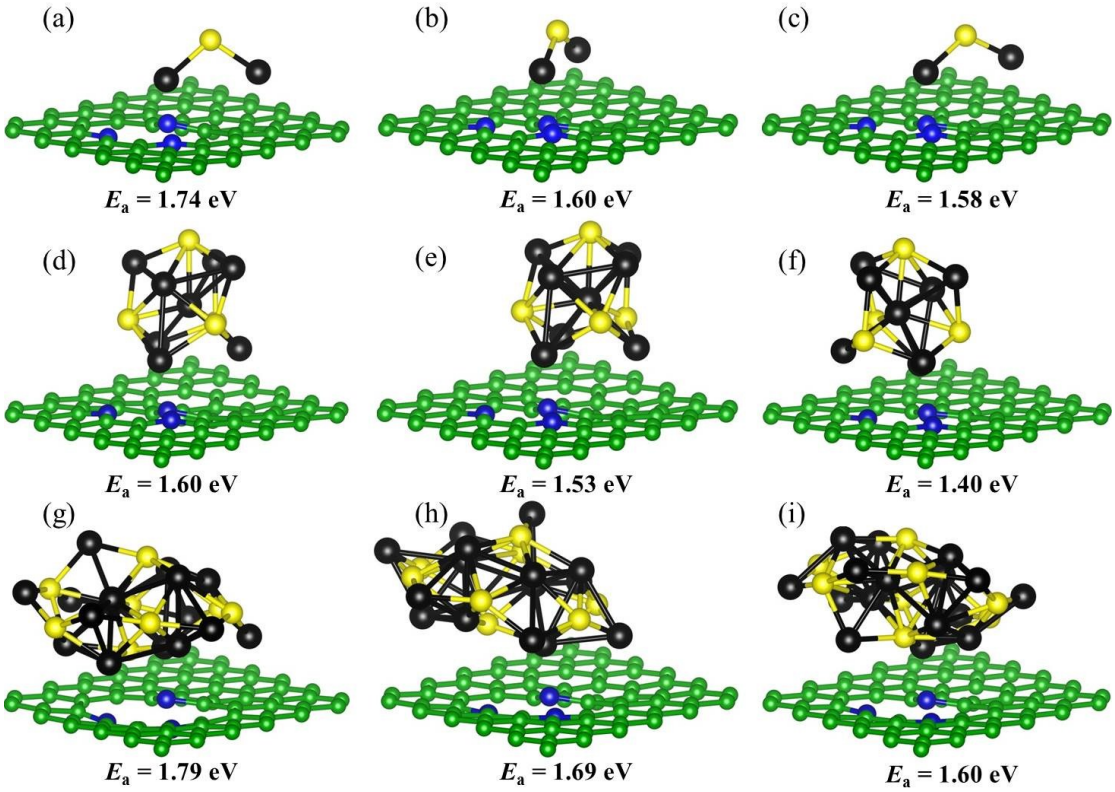

Figure S6. Adsorption configurations and their corresponding adsorption energies on N-doped graphene substrate with 3.1% concentration.

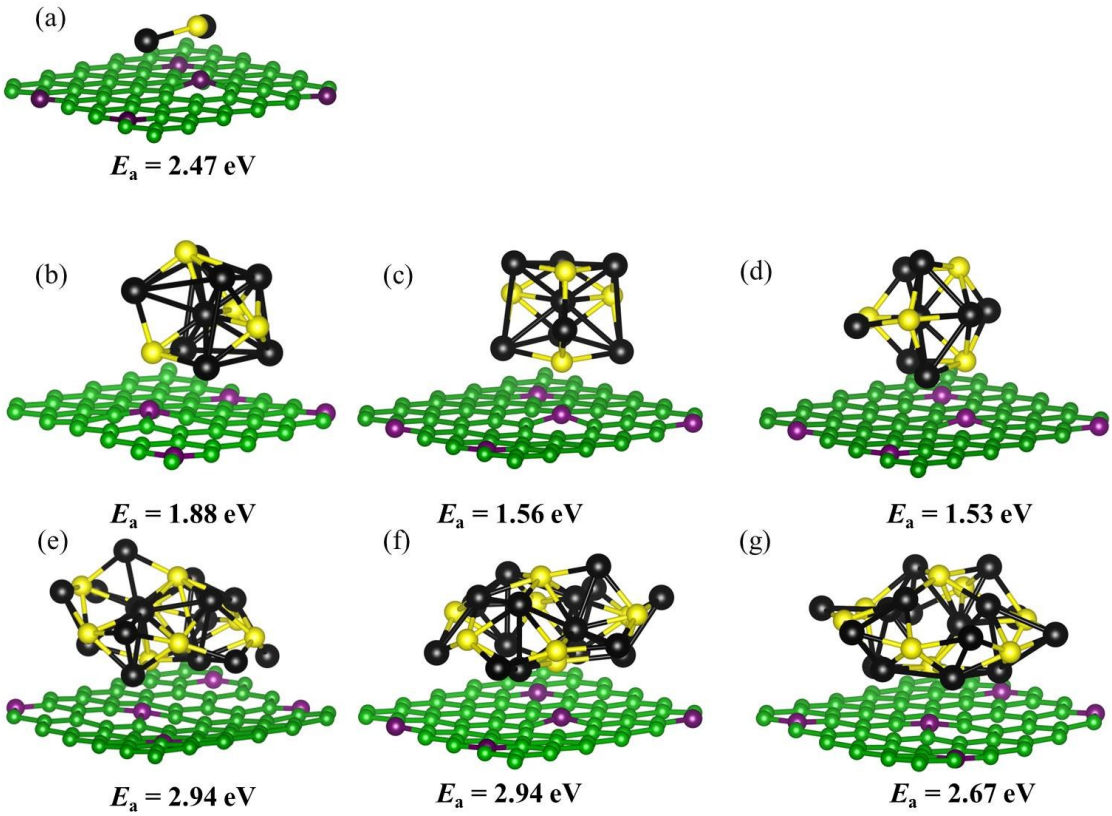

Figure S7. Adsorption configurations and their corresponding adsorption energies on B-doped graphene with 5.2% concentration.

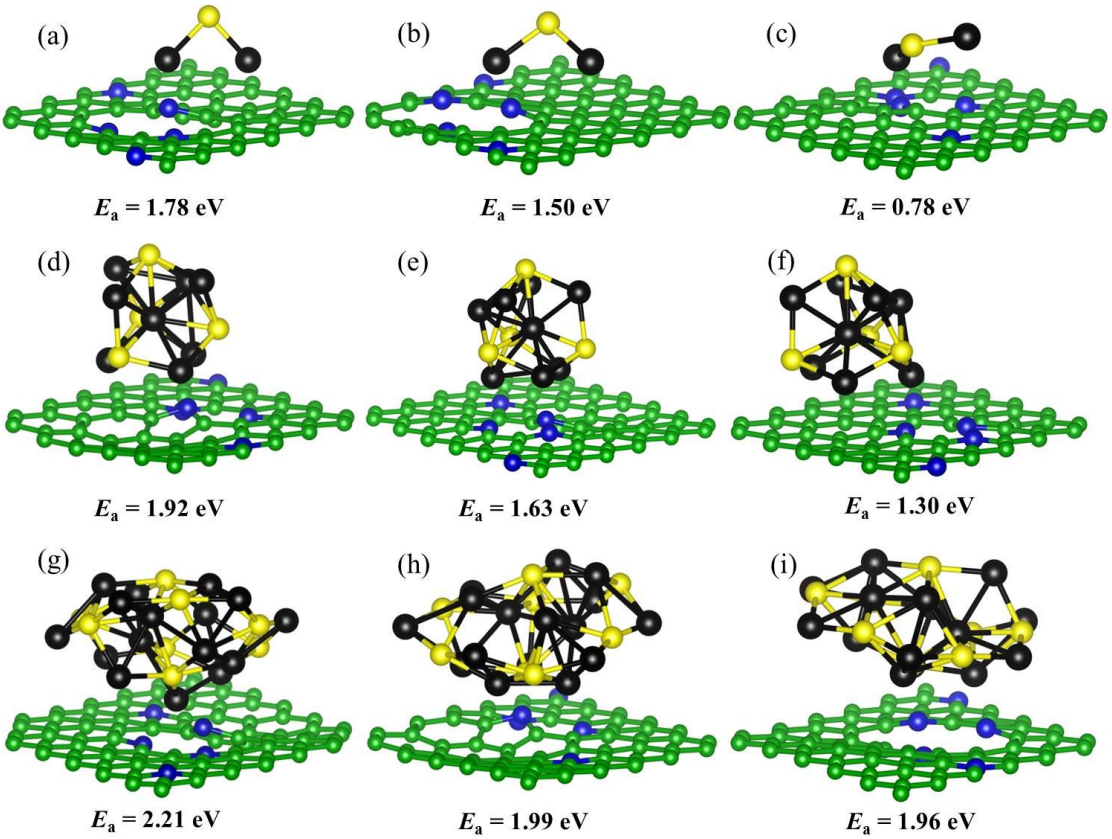

Figure S8. Adsorption configurations and their corresponding adsorption energies on N-doped graphene with 5.2% concentration.

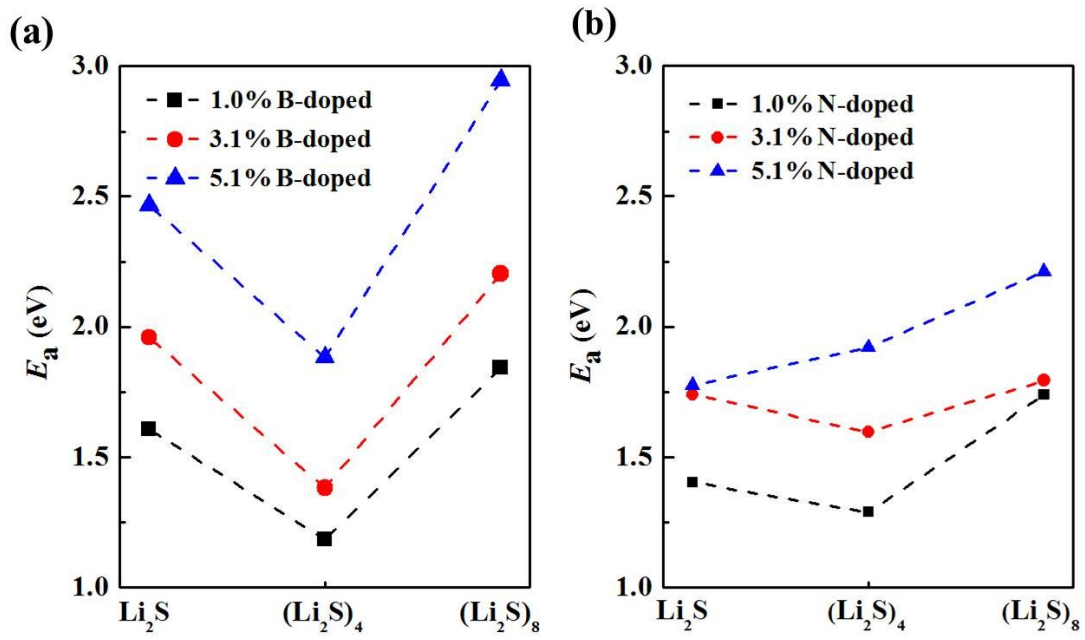

Figure. S9 The adsorption energy (*E*a) variations of Li_2S, $(Li_2S)_4$ and $(Li_2S)_8$ on B-doped graphene, and N-doped graphene with doped concentration of 1%, 3.1%, and 5.2%.

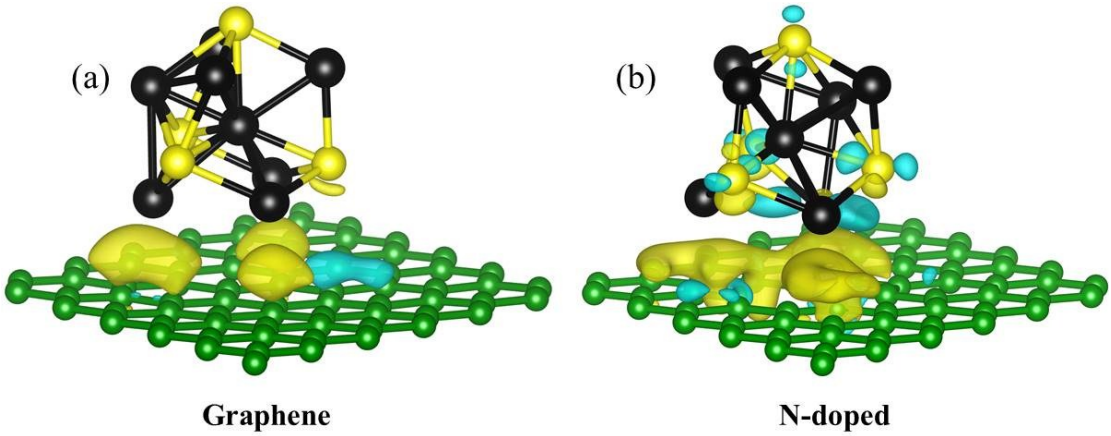

Figure S10. The calculated charge density difference. (a) $(Li_2S)_4$ adsorbed on graphene. (b) $(Li_2S)_4$ adsorbed on N-doped graphene. Charge density difference ($\Delta\rho$) isosurfaces are shown; the cyan and yellow colors indicate the regions of charge loss and gain, respectively. Compared with a and b, there is more charge transfer from $(Li_2S)_4$ to N-doped graphene. Based on the calculated Mulliken charge, $(Li_2S)_4$ transfers 0.70e to N-doped graphene, whereas $(Li_2S)_4$ only transfers 0.27e to graphene.

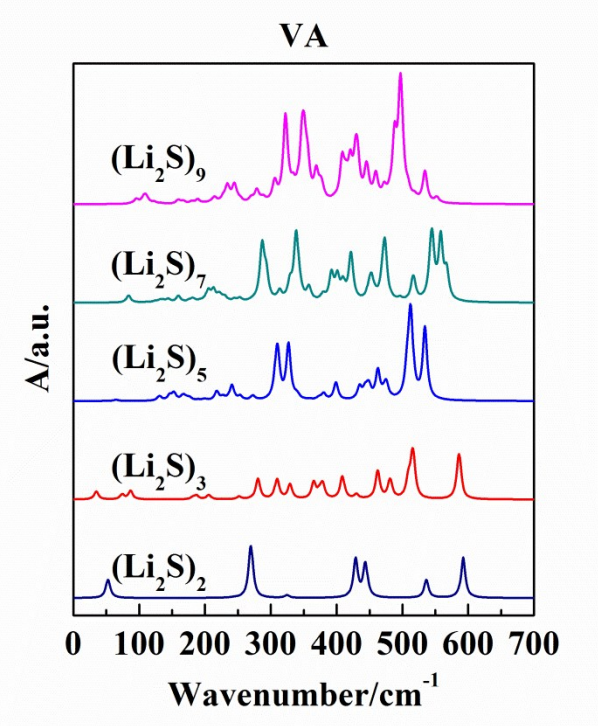

Figure S11. The simulated infrared absorption (IR) spectra of the considered $(Li_2S)_n$ (n = 2, 3, 5, 7, 9) clusters.

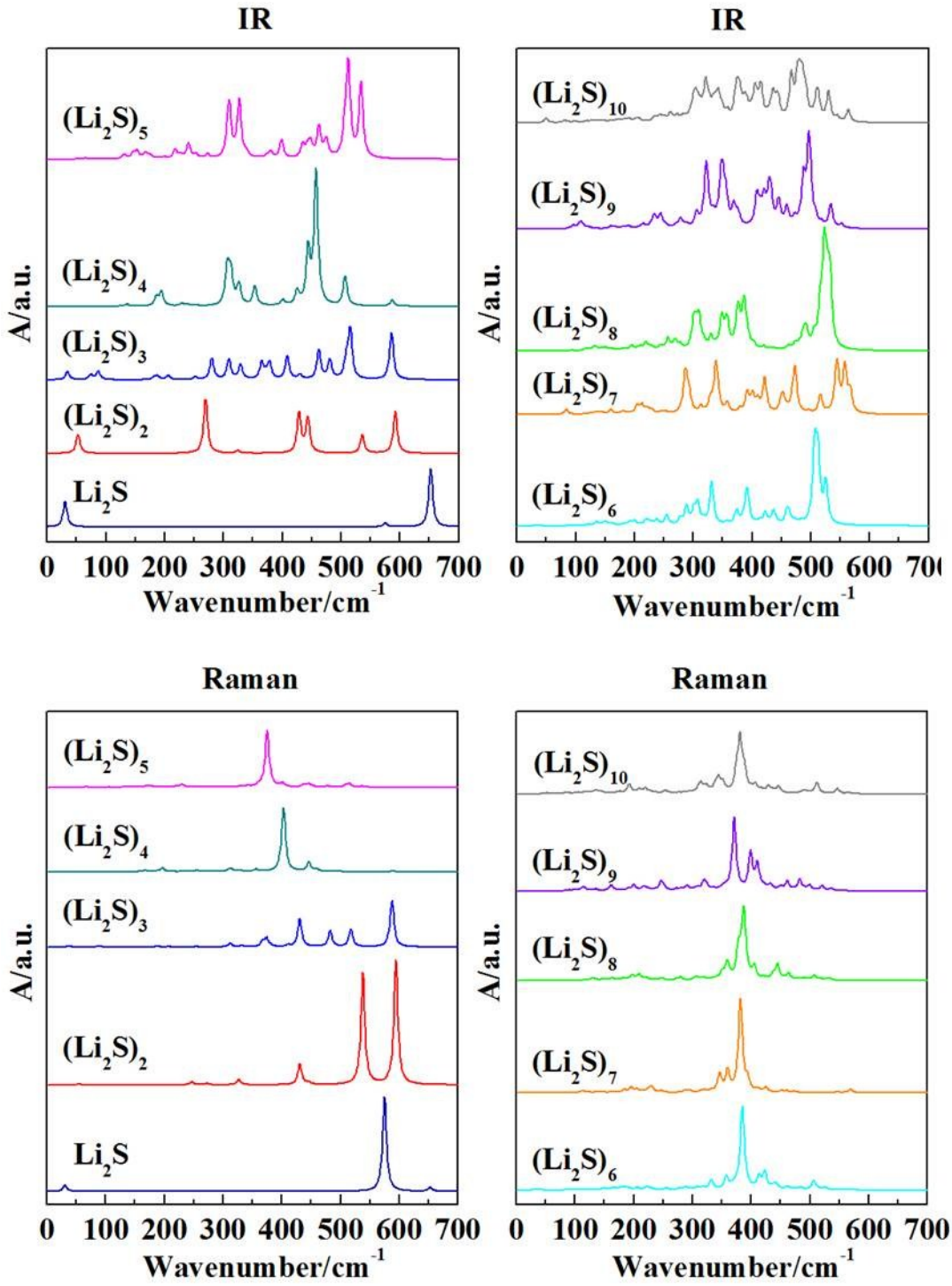

Figure S12. The comparison between the simulated infrared absorption (IR) and Raman spectra.

Table S1. The HOMO-LUMO gap (energy gap) as a function of cluster size *n* for $(Li_2S)_n$, *n* = 1-10.

Cluster size	Energy gap
1	3.13
2	2.65
3	2.68
4	4.27
5	4.11
6	4.10
7	4.44
8	4.28
9	3.92
10	4.25

Table S2. Cartesian Coordinates of Li_2S at B3LYP/6-31+G (*d*) level.

Center Number	Atomic Number	Atomic Type	Coordinates (Angstroms)		
			x	y	z
1	3	0	-1.236708	1.392362	0.018936
2	3	0	0.797059	0.870423	0.018936
3	16	0	-2.407594	3.135248	0.018936

Table S3. Cartesian Coordinates of $(Li_2S)_2$ at B3LYP/6-31+G (*d*) level.

Center Number	Atomic Number	Atomic Type	Coordinates (Angstroms)		
			x	y	z
1	3	0	-0.336788	0.011405	1.483340
2	3	0	-0.338287	-1.290436	-0.732534
3	3	0	3.665247	-0.008306	0.008215
4	3	0	-0.340798	1.281532	-0.750738
5	16	0	1.534360	0.002434	-0.002683
6	16	0	-2.031118	-0.001345	0.001130

Table S4. Cartesian Coordinates of $(Li_2S)_3$ at B3LYP/6-31+G (*d*) level.

Center Number	Atomic Number	Atomic Type	Coordinates (Angstroms)		
			x	y	z
1	3	0	-0.043484	-0.000030	-1.000914
2	3	0	-1.067003	0.000156	1.368666
3	3	0	0.911951	1.970632	0.367663
4	3	0	-2.581238	0.000541	-0.625458

5	3	0	4.127474	0.000640	-0.671843
6	3	0	0.911072	-1.971303	0.367491
7	16	0	2.145577	-0.000610	0.117799
8	16	0	-1.284965	-1.829144	-0.040722
9	16	0	-1.284132	1.829634	-0.040628

Table S5. Cartesian Coordinates of $(Li_2S)_4$ at B3LYP/6-31+G (*d*) level.

Center Number	Atomic Number	Atomic Type	Coordinates (Angstroms)		
			x	y	z
1	3	0	-1.527157	-1.457524	-1.467129
2	3	0	0.917986	1.681356	1.707444
3	3	0	-1.523100	-0.551308	1.995171
4	3	0	0.918252	-2.319102	0.602787
5	3	0	-1.523017	2.004961	-0.518627
6	3	0	-0.205891	0.001562	-0.001370
7	3	0	0.909941	0.636458	-2.312762
8	3	0	2.070856	0.000342	-0.004068
9	16	0	0.839645	2.117936	-0.551745
10	16	0	0.835954	-1.537087	-1.559459
11	16	0	0.839702	-0.582373	2.109260
12	16	0	-2.522402	0.002134	0.001673

Table S6. Cartesian Coordinates of $(Li_2S)_5$ at B3LYP/6-31+G (*d*) level.

Center Number	Atomic Number	Atomic Type	Coordinates (Angstroms)		
			x	y	z
1	3	0	0.338504	-2.062269	1.330377
2	3	0	0.789076	0.000453	-0.088859
3	3	0	2.006112	-1.778757	-1.494421
4	3	0	0.337799	2.062046	1.331181
5	3	0	2.725143	-0.000375	1.616055
6	3	0	2.006696	1.779101	-1.494011
7	3	0	-2.473767	2.073184	-0.511026
8	3	0	-1.729214	-0.000928	1.620884
9	3	0	-2.474328	-2.072927	-0.511913
10	3	0	-1.289926	0.000228	-1.410425
11	16	0	-0.196040	2.130208	-0.895179
12	16	0	3.122944	-0.000144	-0.606964
13	16	0	-3.281533	0.000142	-0.057672
14	16	0	-0.196462	-2.129832	-0.895594
15	16	0	0.506823	-0.000327	2.382689

Table S7. Cartesian Coordinates of $(Li_2S)_6$ at B3LYP/6-31+G (*d*) level.

Center Number	Atomic Number	Atomic Type	Coordinates (Angstroms)		
			x	y	z
1	3	0	2.712510	-1.981521	-0.844991
2	3	0	-1.623921	-2.541931	-1.682887
3	3	0	-1.015877	2.960908	-1.217680
4	3	0	-1.257479	0.002406	-0.672763
5	3	0	3.250034	1.619579	-0.298565
6	3	0	-3.908432	0.233568	-0.395439
7	3	0	1.337349	-0.043110	0.144727
8	3	0	-2.216909	0.000502	1.710766
9	3	0	1.107831	0.367746	-2.425846
10	3	0	-0.258954	1.872541	1.089559
11	3	0	2.348433	-0.512882	2.390843
12	3	0	-0.586147	-2.002062	0.798224
13	16	0	3.662513	-0.455503	0.517446
14	16	0	-2.847908	-1.739397	0.034306
15	16	0	0.506305	-1.680881	-1.570089
16	16	0	0.077957	-0.210595	2.149190
17	16	0	1.112827	2.160512	-1.011631
18	16	0	-2.490777	1.930413	0.144038

Table S8. Cartesian Coordinates of $(Li_2S)_7$ at B3LYP/6-31+G (*d*) level.

Center Number	Atomic Number	Atomic Type	Coordinates (Angstroms)		
			x	y	z
1	3	0	-1.323417	1.687910	1.617359
2	3	0	-2.190667	-0.854479	1.410298
3	3	0	0.000639	-3.692168	0.000231
4	3	0	3.501019	-0.860812	0.790760
5	3	0	1.207527	1.180669	1.128835
6	3	0	-3.500485	-0.861958	-0.791075
7	3	0	0.000353	-1.119627	0.000103
8	3	0	1.322547	1.687994	-1.617266
9	3	0	2.316747	3.303245	0.168753
10	3	0	-2.317855	3.302235	-0.169704
11	3	0	-1.207575	1.179491	-1.127913
12	3	0	1.110530	-1.926711	2.342007
13	3	0	-1.109633	-1.927552	-2.341878
14	3	0	2.190853	-0.853865	-1.410358
15	16	0	0.204239	-0.148494	-2.365853
16	16	0	-0.204268	-0.148302	2.365679
17	16	0	-3.180002	1.176780	0.178041
18	16	0	-2.012400	-2.590892	-0.344785

19	16	0	2.013385	-2.590213	0.344968
20	16	0	3.179470	1.177883	-0.178021
21	16	0	-0.000532	3.077419	-0.000058

Table S9. Cartesian Coordinates of $(Li_2S)_8$ at B3LYP/6-31+G (*d*) level.

Center Number	Atomic Number	Atomic Type	Coordinates (Angstroms)		
			x	y	z
1	3	0	0.155964	-4.223747	0.020836
2	3	0	1.526409	0.494426	0.441419
3	3	0	0.928594	-1.856223	2.369514
4	3	0	-2.348672	1.071402	1.163490
5	3	0	-3.913424	-2.404679	-0.644135
6	3	0	-0.104484	2.329559	1.627320
7	3	0	0.041014	-1.613667	-0.081016
8	3	0	3.885529	-1.737304	0.755939
9	3	0	-2.223730	-1.449435	1.154835
10	3	0	-1.817842	-0.952025	-1.628165
11	3	0	-3.715349	2.073856	-0.741354
12	3	0	2.256153	1.354966	-1.751774
13	3	0	3.733027	2.245636	0.388340
14	3	0	-0.412362	1.874600	-0.988179
15	3	0	-0.141178	4.450886	-0.092874
16	3	0	2.316077	-1.411858	-1.355086
17	16	0	0.409541	-0.105298	-1.897851
18	16	0	-0.388337	-0.050225	1.962864
19	16	0	1.966704	-2.947406	0.623037
20	16	0	-1.794346	-3.160708	-0.381215
21	16	0	-3.752210	-0.160489	-0.304116
22	16	0	-1.990606	3.205228	0.261584
23	16	0	1.619354	3.009352	0.053361
24	16	0	3.898827	0.163348	-0.437497

Table S10. Cartesian Coordinates of $(Li_2S)_9$ at B3LYP/6-31+G (*d*) level.

Center Number	Atomic Number	Atomic Type	Coordinates (Angstroms)		
			x	y	z
1	3	0	-0.192642	-0.473582	-0.001783
2	3	0	1.133503	2.282403	-1.323497
3	3	0	-0.269566	-1.940290	2.169018
4	3	0	3.398370	0.633544	-1.869185
5	3	0	-4.477438	-0.108789	1.750781
6	3	0	3.398807	0.633792	1.869310
7	3	0	-1.047440	0.746338	-2.176946

8	3	0	1.133604	2.282685	1.323381
9	3	0	-1.977952	-2.456249	0.000514
10	3	0	-4.477372	-0.109453	-1.750404
11	3	0	5.062077	1.147763	-0.000253
12	3	0	-3.145258	2.778212	-0.000112
13	3	0	2.342338	-1.960921	1.298985
14	3	0	-1.046903	0.746224	2.175903
15	3	0	2.342334	-1.961108	-1.298500
16	3	0	-2.715260	0.231319	0.000172
17	16	0	2.120409	0.272211	0.000288
18	16	0	-0.269752	-1.941714	-2.169396
19	16	0	1.237764	0.027017	-2.283000
20	16	0	-2.407348	-1.116025	1.952345
21	16	0	4.163923	-0.966833	0.000031
22	16	0	-4.845196	1.300496	-0.000124
23	16	0	-2.407015	-1.116338	-1.951825
24	16	0	3.161972	2.434638	-0.000277
25	16	0	-0.901312	2.081323	-0.000245
26	16	0	0.513014	-2.822246	0.000130
27	16	0	1.238223	0.027521	2.283287

Table S11. Cartesian Coordinates of $(Li_2S)_{10}$ at B3LYP/6-31+G (*d*) level.

Center Number	Atomic Number	Atomic Type	Coordinates (Angstroms)		
			x	y	z
1	3	0	-1.936675	1.513698	1.703828
2	3	0	2.214036	0.825234	1.987617
3	3	0	1.738532	-3.306300	0.449712
4	3	0	-0.004868	-1.182530	0.347833
5	3	0	-1.754965	-1.946418	-1.977472
6	3	0	4.697939	-0.628865	-1.293286
7	3	0	-0.525142	-2.714598	2.075576
8	3	0	-2.685741	-2.585783	0.318511
9	3	0	-1.058091	3.617569	0.294464
10	3	0	3.206239	-1.172243	0.689351
11	3	0	-0.122987	-0.024943	2.956372
12	3	0	0.878066	1.580139	-0.190639
13	3	0	0.943134	-2.545871	-1.901064
14	3	0	2.189021	-0.274940	-1.652863
15	3	0	-0.895614	2.238974	-1.973097
16	3	0	1.490919	3.802451	1.056550
17	3	0	-4.187377	0.956879	-1.679630
18	3	0	2.846643	2.925419	-1.433616
19	16	0	-4.093733	-0.355143	0.873205

20	16	0	-2.069040	0.115923	-0.521963
21	16	0	1.569111	-1.525276	2.227841
22	16	0	3.210613	-2.380995	-1.307228
23	16	0	-0.558837	-3.453074	-0.298547
24	16	0	-3.907139	-1.276144	-1.251415
25	16	0	-2.109210	-0.852488	1.965667
26	16	0	0.289996	2.209039	2.150037
27	16	0	3.488931	1.102656	-0.173448
28	16	0	-0.086733	-0.099349	-1.814388
29	16	0	0.793136	3.815343	-1.147243
30	16	0	-2.853048	2.303040	-0.375537

Reference:

(1) Wang, Y.; Lv, J.; Zhu, L.; Ma, Y. *Phys. Rev. B* **2010**, *82*, 094116.

(2) Wang, Y.; Lv, J.; Zhu, L.; Ma, Y. *Comput. Phys. Commun*. **2012**, *183*, 2063.

(3) Yin, L.; Liang, J.; Zhou, G.; Li, F.; Saito R.; Cheng H. *Nano Eenrgy* **2016**, *25*, 203.